Dislocations and inclusions in prestressed metals

Argani, Luca; Bigoni, Davide; Mishuris, Gennady

Published in:
Proceedings of the Royal Society A: Mathematical, Physical and Engineering Sciences

DOI:
10.1098/rspa.2012.0752

Publication date:
2013

Citation for published version (APA):
Argani, L., Bigoni, D., & Mishuris, G. (2013). Dislocations and inclusions in prestressed metals. *Proceedings of the Royal Society A: Mathematical, Physical and Engineering Sciences*, *469*(2154), [20120752]. https://doi.org/10.1098/rspa.2012.0752

Published in Proceedings of the Royal Society A - 8 June 2013, vol. 469 no. 2154; doi:10.1098/rspa.2012.0752

Dislocations and inclusions in prestressed metals

LUCA PRAKASH ARGANI[1], DAVIDE BIGONI[* 1], AND GENNADY MISHURIS[3]

[1,2]*Department of Civil, Environmental & Mechanical Engineering, University of Trento, via Mesiano 77, I-38123 Trento, Italy*

[3]*Department of Mathematics and Physics, University of Wales, Aberystwyth, UK*

Abstract

The effect of prestress on dislocation (and inclusion) fields in nonlinear elastic solids is analysed by extending previous solutions by Eshelby and Willis. Employing a plane strain constitutive model (for incompressible incremental nonlinear elasticity) to describe the behaviour of ductile metals (the J_2–deformation theory of plasticity), we show that when the level of prestress is high enough that shear band formation is approached, strongly localized strain patterns emerge, when a dislocation dipole is emitted by a source. These may explain cascade activation of dislocation clustering along slip band directions.

Keywords: Inclusions; prestress; nonlinear elasticity; singular solutions; Green's functions.

1 Introduction

The theory of dislocations (and inclusions) in solids has been thoroughly developed for elastic materials, unloaded in their natural state. We extend this theory to cover the possibility that the material is prestressed, through a generalization of solutions found by Eshelby [1–3] and Willis [4], by introducing an incremental formulation for incompressible materials, in which the nominal stress is related to the incremental displacement gradient, within a constitutive framework (which embraces Mooney-Rivlin and Ogden materials and also material models describing softening [5]) under the plane strain constraint, even if several of the presented results remain valid within a three-dimensional context.

Anisotropy strongly influences near dislocation stress fields (as shown in Figure 1; see Appendix A for details) and almost all crystals are anisotropic, so that anisotropy has been the subject of an intense research effort [6–8] and has been recently advocated as a way to study dislocation core properties [9, 10].

Our interest is to analyse the effect of orthotropy induced by prestress on dislocation (and inclusions) fields, within the general framework of incremental nonlinear elasticity, but with a special emphasis on a material model for metals (the J_2–deformation theory [11, 12]), so that our investigation is addressed to ductile metals subject to extreme strain, where the nucleation of a clustering of dislocations into a 'super dislocation' perturbs a material that has a low stiffness, so low that the differential equations governing the incremental equilibrium are close to the boundary of ellipticity loss.

When this boundary is approached (from the interior of the elliptic region), our solution for edge dislocations (but also, in general, for inclusions) reveals features of severely deformed

*Corresponding author: e-mail: bigoni@ing.unitn.it ; phone: +39 0461 282507; web-page: www.ing.unitn.it/~bigoni/

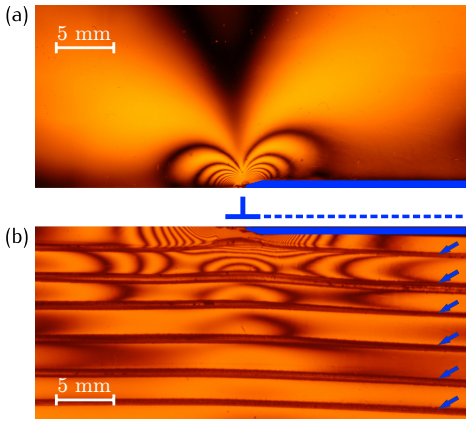

Figure 1: Photoelasticity (in monochromatic light) discloses the stress field (in-plane principal stress difference) around an edge dislocation (as sketched) in an isotropic material (**a**) and in an orthotropic material (**b**) (with orthotropy axes aligned parallel and orthogonal to the dislocation line). Orthotropy has been simulated by cutting parallel groves (indicated with arrows) in a photoelastic $5\,\mathrm{mm}$ thick) two-component resin, in which two parallel metallic ($0.5\,\mathrm{mm}$ thick) steel laminae simulate a dislocation, when forced to slide one against the other. Compared with the isotropic case (**a**), the fields become strongly elongated along the orthotropy axis parallel to the dislocation for anisotropy (**b**).

metals near the shear band formation. In this situation we show that emission of a dislocation (which can be also viewed as a 'super dislocation') dipole produces incremental fields strongly localized along the directions of the shear bands, formally excluded *within* the elliptic region. This may induce a cascade of dislocation clustering, which may explain the fact that the amount of slip that takes place on an active shear band is three orders of magnitude greater than could be produced by the passage of a single dislocation [13].

This paper is organized as follows. A boundary integral equation, proposed by Eshelby [2] and Willis [4] for *an inclusion in an infinite plane subject to a generic transformation strain*, is generalized in Section 2 to incremental, incompressible nonlinear elasticity in plane strain (for a uniformly prestressed material), and a new boundary equation is formulated for the in-plane incremental mean stress (when the prestress is set to be equal to zero, our generalization reduces for isotropic incompressible material to novel formulae because the incompressible case has never been explicitly addressed). As an example of application of the derived equations, we present the case of a circular inclusion subject to a uniform purely dilatational transformation strain. This solution, in the case of the J_2–deformation theory of plasticity, shows the strong effect of prestress, particularly when the material is prestressed near the boundary of ellipticity loss. In Section 3, the solution for an edge dislocation incrementally deformed within a uniformely prestressed elastic material is derived and, after treatment of the boundary integral equations in view of the numerical implementation (Section 4), applications are presented in Section 5, where a dislocation dipole (different from a force dipole, see Bigoni [14] for a discussion on the differences) is emitted within the J_2–deformation theory of plasticity material homogeneously deformed near the elliptic boundary.

2 Inclusions in prestressed elastic materials

2.1 Material model

We refer to an incompressible nonlinear elastic material deformed under plane strain condition in the x_1–x_2 reference system, whereas x_3 represents the out-of-plane direction. Under these hypotheses, and assuming the current configuration as the reference configuration, the most

general material model has been provided by Biot [15], which in the Bigoni & Dal Corso [16] notation, can be written as a linear relation between the increment in the nominal (asymmetric) stress $\dot{t}_{ij}$ and the incremental displacement v_i (plus the incompressibility constraint) as

$$\dot{t}_{ij} = \mathbb{K}_{ijkl} v_{l,k} + \dot{p}\delta_{ij}\,, \qquad v_{k,k} = 0\,, \tag{1}$$

where repeated indices are summed between 1 and 2, δ_{ij} is the Kronecker delta, $\dot{p}$ is the increment in the in-plane mean stress and the non-null components of the fourth-order tensor $\mathbb{K}$ are

$$\begin{aligned}
&\mathbb{K}_{1111} = \mu_* - \frac{\sigma}{2} - p\,, && \mathbb{K}_{1122} = \mathbb{K}_{2211} = -\mu_*\,,\\
&\mathbb{K}_{2222} = \mu_* + \frac{\sigma}{2} - p\,, && \mathbb{K}_{1221} = \mathbb{K}_{2112} = \mu - p\,,\\
&\mathbb{K}_{1212} = \mu + \frac{\sigma}{2}\,, && \mathbb{K}_{2121} = \mu - \frac{\sigma}{2}\,,
\end{aligned} \tag{2}$$

which are functions of the dimensionless prestress and anisotropy parameters

$$\xi = \frac{\mu_*}{\mu}\,, \qquad \eta = \frac{p}{\mu} = \frac{\sigma_1+\sigma_2}{2\mu}\,, \qquad k = \frac{\sigma}{2\mu} = \frac{\sigma_1-\sigma_2}{2\mu}\,. \tag{3}$$

Within this framework, μ and μ_* are, respectively, the incremental shear moduli parallel to, and inclined at $45°$ to, the principal stress axes. For the Mooney-Rivlin material, these moduli depend on the maximum current stretch $\lambda > 1$ and are expressed as [14]

$$\mu = \mu_* = \frac{\mu_0}{2}\left(\lambda^2 + \lambda^{-2}\right), \tag{4}$$

with μ_0 the ground-state shear modulus, whereas for the Ogden material, the definitions are the following:

$$\mu_* = \frac{1}{4}\sum_{i=1}^{N} \mu_i\,\beta_i\left(\lambda^{\beta_i} + \lambda^{-\beta_i}\right), \qquad \mu = \frac{1}{2}\frac{\lambda^4+1}{\lambda^4-1}\sum_{i=1}^{N} \mu_i\left(\lambda^{\beta_i} + \lambda^{-\beta_i}\right), \tag{5}$$

where μ_i and β_i are material parameters.

We will restrict the analysis to the elliptic regime, which corresponds to

$$\mu > 0\,, \qquad k^2 < 1\,, \qquad 2\xi > 1 - \sqrt{1-k^2}\,, \tag{6}$$

and may be further subdivided into elliptic complex region,

$$\mu > 0\,, \qquad k^2 < 1\,, \qquad 1 - \sqrt{1-k^2} < 2\xi < 1 + \sqrt{1-k^2}\,, \tag{7}$$

and elliptic imaginary region,

$$\mu > 0\,, \qquad k^2 < 1\,, \qquad 2\xi > 1 + \sqrt{1-k^2}\,. \tag{8}$$

A special case of the above constitutive framework is the J_2–deformation theory of plasticity, proposed by Hutchinson & Neale [11], in which

$$k = \tanh(2\widehat{\varepsilon})\,, \qquad \xi = \frac{Nk}{2\widehat{\varepsilon}}\,, \tag{9}$$

where $\widehat{\varepsilon} = \log\lambda \geq 0$ (λ is the in-plane maximum stretch) is the logarithmic strain and N is an hardening parameter $\in (0,1)$, so that a vanishing N corresponds to ideal plastic behaviour.

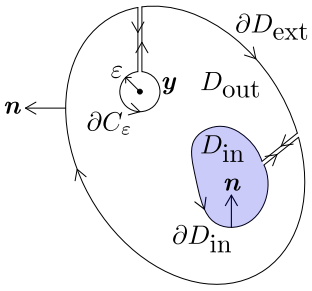

Figure 2: Integration domain D_{out} for an infinite body containing an inclusion (shown in grey) of volume D_{in} and surface ∂D_{in}; the singularity at $\boldsymbol{y}$ is enclosed in a disk C_ε of radius ε and surface ∂C_ε. D_{out} represents the simply connected region outside the inclusion and excluding the disk surrounding the singularity, whereas its external boundary is represented by ∂D_{ext}.

This material touches the elliptic-hyperbolic boundary when the logarithmic strain reaches the critical value $\widehat{\varepsilon}^{\text{E}}$ solution of

$$\widehat{\varepsilon}^{\text{E}} \tanh\left(\widehat{\varepsilon}^{\text{E}}\right) = N \,, \tag{10}$$

so that, for instance, $N = 0.4$ yields $\widehat{\varepsilon}^{\text{E}} = 0.678$.

2.2 The inclusion problem

We follow and generalize Eshelby [2] and Willis [4] by considering an infinite elastic plane, homogeneously prestressed and incompressible and therefore obeying the incremental constitutive laws (1), containing an inclusion of arbitrary shape, in which a uniform incremental displacement gradient $v^{\text{P}}_{i,j}$ is prescribed, which can be thought as an inelastic (e.g. plastic or thermal) deformation.

Note that the Eshelby inclusion problem in linear elasticity is formulated by prescribing an inelastic *strain*, not a displacement gradient (if a displacement gradient is assigned instead, the skew symmetric part of this, representing a rigid-body infinitesimal rotation, produces null fields outside the inclusion, meaning that the solution for the infinite body containing the inclusion consists of a pure, uniform, rigid-body rotation), a situation different from incremental nonlinear elasticity, where the effect of prestress is to alter the incremental response, even for a rigid-body rotation.

Because the inclusion is constrained by the surrounding matrix material, an elastic deformation $v^{\text{E}}_{i,j}$ is produced, so that the 'total' incremental displacement gradient $v_{i,j}$ within the inclusion can be obtained through the additive rule

$$v_{i,j} = v^{\text{E}}_{i,j} + v^{\text{P}}_{i,j} \,. \tag{11}$$

It is important to note that, although the material is incompressible, *the prescribed inelastic incremental displacement* v^{P}_i *need not satisfy the incompressibility constraint*, so that, since v^{E}_i does (namely $v^{\text{E}}_{k,k} = 0$), it follows that $v_{k,k} = v^{\text{P}}_{k,k}$.

The elastic part of the incremental deformation produces the incremental nominal stress

$$\dot{t}_{ij} = \mathbb{K}_{ijkl} v_{l,k} - \mathbb{K}_{ijkl} v^{\text{P}}_{l,k} + \dot{p}\,\delta_{ij} - \dot{p}^{\text{P}}\delta_{ij} \,, \tag{12}$$

through two incremental mean stresses $\dot{p}$ and $\dot{p}^{\text{P}}$, the latter being a homogeneous incremental mean stress, defined inside the inclusion and associated to the deformation $v^{\text{P}}_{i,j}$ (we will show later that results will be independent of this, but it is better for the moment to keep track of a part of the stress that is related to the inclusion transformation).

Body forces are not considered, so that the incremental nominal stress has to satisfy the

equilibrium equations, which for an infinite body containing a concentrated unit force can be written as

$$\frac{\partial\, \dot{t}^g_{ij}(\boldsymbol{x}-\boldsymbol{y})}{\partial\, x_i} + \delta_{gj}\delta(\boldsymbol{x}-\boldsymbol{y}) = 0\,, \tag{13}$$

where $\dot{t}^g_{ij}$ is the Green's function for incremental nominal stress, in other words, the ij-component of the nominal stress at $\boldsymbol{x}$ produced by a unit point force applied in the g-direction at a point $\boldsymbol{y}$, and $\delta(\boldsymbol{x}-\boldsymbol{y})$ is the Dirac delta. This Green's function, valid within the present constitutive framework, has been given by Bigoni & Capuani [17].

2.2.1 The incremental displacement

We consider now the inclusion problem sketched in Figure 2, where an inclusion of volume D_{in} and surface ∂D_{in} is included in an infinite region. We assume that the singularity at point $\boldsymbol{y}$ is enclosed by a disk C_ε centred in $\boldsymbol{y}$, with radius ε and surface ∂C_ε. We define a closed, finite and simply connected domain D_{out} outside both the inclusion and the disk surrounding the singularity at $\boldsymbol{y}$, so that its boundary ∂D_{out} can be regarded as the union of the surfaces of inclusion and disk (∂D_{in} and ∂C_ε) and an external boundary ∂D_{ext} as follows:

$$\partial D_{\text{out}} = \partial D_{\text{in}} \cup \partial C_\varepsilon \cup \partial D_{\text{ext}}\,. \tag{14}$$

On the above defined region, D_{out}, we may use the Betti identity, thus yielding

$$\int_{D_{\text{out}}} \left[\dot{t}^g_{ij,i}(\boldsymbol{x}-\boldsymbol{y})v_j(\boldsymbol{x}) - \dot{t}_{ij,i}(\boldsymbol{x})v^g_j(\boldsymbol{x}-\boldsymbol{y})\right] \mathrm{d}V_{\boldsymbol{x}} = 0\,, \tag{15}$$

where the comma denotes differentiation with respect to $\boldsymbol{x}$, the same variable for which integration is performed (as noted by the symbol $\mathrm{d}V_{\boldsymbol{x}}$), and $v^g_j(\boldsymbol{x}-\boldsymbol{y})$ is the infinite-body Green's function for incremental displacements [17].

Using the rule of product differentiation, equation (15) becomes

$$\int_{D_{\text{out}}} \frac{\partial}{\partial x_i}\left[\dot{t}^g_{ij}(\boldsymbol{x}-\boldsymbol{y})v_j(\boldsymbol{x}) - \dot{t}_{ij}(\boldsymbol{x})v^g_j(\boldsymbol{x}-\boldsymbol{y})\right] \mathrm{d}V_{\boldsymbol{x}}\,, \tag{16}$$

because the quantity

$$\dot{t}^g_{ij}(\boldsymbol{x}-\boldsymbol{y})v_{j,i}(\boldsymbol{x}) - \dot{t}_{ij}(\boldsymbol{x})v^g_{j,i}(\boldsymbol{x}-\boldsymbol{y}), \tag{17}$$

is equal to zero, owing to the major symmetry of $\mathbb{K}_{ijkl}$ and the incompressibility constraint ($v_{k,k} = v^g_{k,k} = 0$). On application of the divergence theorem to equation (16) it follows that:

$$\int_{\partial D_{\text{out}}} \left[\dot{t}^g_{ij}(\boldsymbol{x}-\boldsymbol{y})v_j(\boldsymbol{x}) - \dot{t}_{ij}(\boldsymbol{x})v^g_j(\boldsymbol{x}-\boldsymbol{y})\right] n_i \,\mathrm{d}S_{\boldsymbol{x}} = 0\,, \tag{18}$$

where n_i is the unit vector normal to the integration boundary and pointing towards the external of the domain (Figure 2).

Recalling equation (14), the integration regions given by the domain D_{out} and the contour ∂D_{out} can be split. Since $v^g_i \sim \log r$, we can write

$$\lim_{\varepsilon\to 0}\int_{\partial C_\varepsilon} \dot{t}_{ij}(\boldsymbol{x})v^g_j(\boldsymbol{x}-\boldsymbol{y})n_i \,\mathrm{d}S_{\boldsymbol{x}} = 0\,, \tag{19}$$

whereas

$$\lim_{\varepsilon\to 0}\int_{\partial C_\varepsilon} \dot{t}^g_{ij}(\boldsymbol{x})v_j(\boldsymbol{x}-\boldsymbol{y})n_i \,\mathrm{d}S_{\boldsymbol{x}} = v_g(\boldsymbol{y})\,, \tag{20}$$

is a limit that can be obtained from equation (13) using the delta function properties. Therefore, assuming that the incremental stress and displacement fields induced by the inclusion decay at infinity, where the outer boundary is moved, and for $\varepsilon \to 0$, the integral equation (18) becomes

$$v_g(\boldsymbol{y}) = \int_{\partial D_{\text{in}}} \left[\dot{t}^g_{ij}(\boldsymbol{x}-\boldsymbol{y}) v_j(\boldsymbol{x}) - \dot{t}_{ij}(\boldsymbol{x}) v^g_j(\boldsymbol{x}-\boldsymbol{y}) \right] n_i \, \mathrm{d}S_{\boldsymbol{x}} \,, \tag{21}$$

where now n_i is the outward unit normal to the inclusion surface ∂D_{in}.

A further application of the divergence theorem yields

$$v_g(\boldsymbol{y}) = \int_{D_{\text{in}}} \left[\dot{t}^g_{ij}(\boldsymbol{x}-\boldsymbol{y}) v_{j,i}(\boldsymbol{x}) - \dot{t}_{ij}(\boldsymbol{x}) v^g_{j,i}(\boldsymbol{x}-\boldsymbol{y}) \right] \mathrm{d}V_{\boldsymbol{x}} \,, \tag{22}$$

but within the inclusion the gradient of the velocity can be written as

$$v_{i,j} = v^{\mathrm{E}}_{i,j} + \frac{1}{3} v^{\mathrm{P}}_{k,k} \delta_{ij} \,, \tag{23}$$

so that, using equation (12), we may write

$$v_g(\boldsymbol{y}) = \int_{D_{\text{in}}} \left[\mathbb{K}_{ijkl} v^{\mathrm{P}}_{l,k}(\boldsymbol{x}) v^g_j(\boldsymbol{x}-\boldsymbol{y}) + \dot{p}^g(\boldsymbol{x}-\boldsymbol{y}) v^{\mathrm{P}}_{k,k}(\boldsymbol{x}) \right] \mathrm{d}V_{\boldsymbol{x}} \,, \tag{24}$$

where $\dot{p}^g(\boldsymbol{x}-\boldsymbol{y})$ is the Green's incremental in-plane mean stress, defined in Bigoni & Capuani [17]. Because the field $\dot{p}^{\mathrm{P}}$ is uniform and the incremental displacement field solenoidal, the application of the divergence theorem to the first term of equation (24) yields an *integral equation for the incremental displacements outside the inclusion produced by the uniform inelastic field* $v^{\mathrm{P}}_{l,k}$

$$v_g(\boldsymbol{y}) = \int_{\partial D_{\text{in}}} \mathbb{K}_{ijkl} v^{\mathrm{P}}_{l,k}(\boldsymbol{x}) v^g_j(\boldsymbol{x}-\boldsymbol{y}) n_i \, \mathrm{d}S_{\boldsymbol{x}} + \int_{D_{\text{in}}} \dot{p}^g(\boldsymbol{x}-\boldsymbol{y}) v^{\mathrm{P}}_{k,k}(\boldsymbol{x}) \, \mathrm{d}V_{\boldsymbol{x}} \,. \tag{25}$$

Note that equation (25) involves both the deviatoric and the volumetric part of $v^{\mathrm{P}}_{l,k}$ and that the volumetric term vanishes for purely deviatoric inelastic incremental displacement gradient.

If we introduce a potential $P^g_i(\boldsymbol{x}-\boldsymbol{y})$ such that

$$\dot{p}^g(\boldsymbol{x}-\boldsymbol{y}) = \frac{\partial P^g_i(\boldsymbol{x}-\boldsymbol{y})}{\partial x_i} \,, \tag{26}$$

equation (25) can be rewritten as

$$v_g(\boldsymbol{y}) = \int_{\partial D_{\text{in}}} \left[\mathbb{K}_{ijkl} v^{\mathrm{P}}_{l,k}(\boldsymbol{x}) v^g_j(\boldsymbol{x}-\boldsymbol{y}) + P^g_i(\boldsymbol{x}-\boldsymbol{y}) v^{\mathrm{P}}_{k,k} \right] n_i \, \mathrm{d}S_{\boldsymbol{x}} \,, \tag{27}$$

showing that now the velocity field is expressed only in terms of a boundary integral.

A simple way to calculate $P^g_i(\boldsymbol{x}-\boldsymbol{y})$ is as follows. Within the two-dimensional framework, we may introduce the coefficient $R_i(\hat{\alpha})$ as

$$R_i(\hat{\alpha}) = \delta_{i1}\hat{\alpha} + (1-\hat{\alpha})\delta_{i2} \,, \tag{28}$$

where δ_{ij} is the Kronecker delta, $i,j = 1,2$ and $\hat{\alpha} \in [0,1]$, so that we can obtain a family of potentials $P^g_i(\boldsymbol{x}-\boldsymbol{y})$ depending on the arbitrary coefficient $\hat{\alpha} \in [0,1]$ in the form

$$P^g_i(\boldsymbol{x}-\boldsymbol{y}) = R_i(\hat{\alpha}) \int \dot{p}^g(\boldsymbol{x}-\boldsymbol{y}) \, \mathrm{d}x_i \,, \tag{29}$$

where the index i is *not* summed.

Following Willis [4], we are now in a position to derive an expression that is alternative, but equivalent, to (25). This can be carried out through application of the divergence theorem, so that, collecting the derivative with respect to x_l, we obtain

$$v_g(\boldsymbol{y}) = \int_{D_{\text{in}}} \left[\frac{\partial}{\partial x_k} \left[\mathbb{K}_{ijkl} v_l^{\text{P}} v_{j,i}^g(\boldsymbol{x}-\boldsymbol{y}) \right] - \mathbb{K}_{ijkl} v_l^{\text{P}} v_{j,ik}^g(\boldsymbol{x}-\boldsymbol{y}) + \dot{p}^g(\boldsymbol{x}-\boldsymbol{y}) v_{m,m}^{\text{P}} \right] \mathrm{d}V_{\boldsymbol{x}} \,, \tag{30}$$

an expression that can be transformed using incremental equilibrium, and the major symmetry of $\mathbb{K}$ in the form

$$\mathbb{K}_{ijkl} v_l^{\text{P}} v_{j,ki}^g(\boldsymbol{x}-\boldsymbol{y}) = -\dot{p}_{,l}^g(\boldsymbol{x}-\boldsymbol{y}) v_l^{\text{P}} \,, \tag{31}$$

to yield

$$v_g(\boldsymbol{y}) = \int_{D_{\text{in}}} \left[\frac{\partial}{\partial x_k} \left[\mathbb{K}_{ijkl} v_l^{\text{P}} v_{j,i}^g(\boldsymbol{x}-\boldsymbol{y}) \right] + v_l^{\text{P}} \frac{\partial \dot{p}^g(\boldsymbol{x}-\boldsymbol{y})}{\partial x_l} + \dot{p}^g(\boldsymbol{x}-\boldsymbol{y}) v_{m,m}^{\text{P}} \right] \mathrm{d}V_{\boldsymbol{x}} \,. \tag{32}$$

A second application of the divergence theorem allows us to obtain an *integral equation for the incremental displacements outside the inclusion produced by the uniform inelastic field* $v_{l,k}^{\text{P}}$, fully equivalent to (25),

$$v_g(\boldsymbol{y}) = \int_{\partial D_{\text{in}}} \left[\mathbb{K}_{ijkl} v_{j,i}^g(\boldsymbol{x}-\boldsymbol{y}) + \dot{p}^g(\boldsymbol{x}-\boldsymbol{y}) \delta_{kl} \right] v_l^{\text{P}} n_k \, \mathrm{d}S_{\boldsymbol{x}} \,, \tag{33}$$

and expressed in terms of transformation incremental inelastic displacement v_m^{P}.

Introducing the following notation for the Green's incremental tractions along the surface of unit normal n_i

$$\tau_j^g(\boldsymbol{x}-\boldsymbol{y}) = \dot{t}_{ij}^g(\boldsymbol{x}-\boldsymbol{y}) n_i \,, \tag{34}$$

equation (33) becomes

$$v_g(\boldsymbol{y}) = \int_{\partial D_{\text{in}}} \tau_m^g(\boldsymbol{x}-\boldsymbol{y}) v_m^{\text{P}} \, \mathrm{d}S_{\boldsymbol{x}} \,. \tag{35}$$

Note that the expression for the components of τ_j^g are given both in singular and regularized forms by Bigoni *et al*. [18], and can be used to evaluate the integral equation (35).

The gradient of incremental displacement can be given by two expressions, one when equation (25) is used,

$$\frac{\partial v_g(\boldsymbol{y})}{\partial y_r} = -\int_{\partial D_{\text{in}}} \mathbb{K}_{ijkl} v_{l,k}^{\text{P}} v_{j,r}^g(\boldsymbol{x}-\boldsymbol{y}) n_i \, \mathrm{d}S_{\boldsymbol{x}} - \int_{D_{\text{in}}} \dot{p}_{,r}^g(\boldsymbol{x}-\boldsymbol{y}) v_{m,m}^{\text{P}} \, \mathrm{d}V_{\boldsymbol{x}} \,, \tag{36}$$

and the other when equation (33) is used,

$$\frac{\partial v_g(\boldsymbol{y})}{\partial y_r} = -\int_{\partial D_{\text{in}}} \left[\mathbb{K}_{ijkl} v_{j,ir}^g(\boldsymbol{x}-\boldsymbol{y}) + \dot{p}_{,r}^g(\boldsymbol{x}-\boldsymbol{y}) \delta_{kl} \right] v_l^{\text{P}} n_k \, \mathrm{d}S_{\boldsymbol{x}} \,. \tag{37}$$

According to the two representations (36) and (37), the second gradient can be expressed as

$$\frac{\partial^2 v_g(\boldsymbol{y})}{\partial y_r \partial y_s} = \int_{\partial D_{\text{in}}} \mathbb{K}_{ijkl} v_{l,k}^{\text{P}} v_{j,rs}^g(\boldsymbol{x}-\boldsymbol{y}) n_i \, \mathrm{d}S_{\boldsymbol{x}} + \int_{D_{\text{in}}} \dot{p}_{,rs}^g(\boldsymbol{x}-\boldsymbol{y}) v_{m,m}^{\text{P}} \, \mathrm{d}V_{\boldsymbol{x}} \,, \tag{38}$$

or as

$$\frac{\partial^2 v_g(\boldsymbol{y})}{\partial y_r \partial y_s} = \int_{\partial D_{\text{in}}} \left[\mathbb{K}_{ijkl} v_{j,irs}^g(\boldsymbol{x}-\boldsymbol{y}) + \dot{p}_{,rs}^g(\boldsymbol{x}-\boldsymbol{y}) \delta_{kl} \right] v_l^{\text{P}} n_k \, \mathrm{d}S_{\boldsymbol{x}} \,, \tag{39}$$

because $v^{\mathrm{P}}_{l,kr} = v^{\mathrm{P}}_{l,krs} = 0$, as $v^{\mathrm{P}}_{l,k}$ is homogeneous.

2.2.2 The incremental mean stress

To complete the solution, the incremental mean stress $\dot{p}(\boldsymbol{y})$ has to be calculated. For this purpose, taking into account that $v^{\mathrm{P}}_{m,m}$ is homogeneous, the incremental equilibrium equations (1) allow us to derive the gradient of $\dot{p}$ in the form

$$\dot{p}_{,j} = -\mathbb{K}_{ijkl} v_{l,ik}\,, \tag{40}$$

where the differentiation is carried out with respect to the variable x_i.

Using equation (38) into equation (40), we obtain

$$\frac{\partial \dot{p}(\boldsymbol{y})}{\partial y_i} = -\int_{\partial D_{\mathrm{in}}} \mathbb{K}_{sirg}\mathbb{K}_{jklm} v^{\mathrm{P}}_{m,l} v^{g}_{k,rs}(\boldsymbol{x}-\boldsymbol{y}) n_j \,\mathrm{d}S_{\boldsymbol{x}} - \int_{D_{\mathrm{in}}} \mathbb{K}_{sirg}\dot{p}^{g}_{,rs}(\boldsymbol{x}-\boldsymbol{y}) v^{\mathrm{P}}_{m,m}\,\mathrm{d}V_{\boldsymbol{x}}\,, \tag{41}$$

which, using the rate equilibrium equations (1), yields

$$\frac{\partial \dot{p}(\boldsymbol{y})}{\partial y_i} = \int_{\partial D_{\mathrm{in}}} \mathbb{K}_{jklm} v^{\mathrm{P}}_{m,l} \dot{p}^{k}_{,i}(\boldsymbol{x}-\boldsymbol{y}) n_j \,\mathrm{d}S_{\boldsymbol{x}} - \int_{D_{\mathrm{in}}} \mathbb{K}_{sirg}\dot{p}^{g}_{,rs}(\boldsymbol{x}-\boldsymbol{y}) v^{\mathrm{P}}_{m,m}\,\mathrm{d}V_{\boldsymbol{x}}\,. \tag{42}$$

Defining the function $F(\boldsymbol{x}-\boldsymbol{y})$ as

$$F(\boldsymbol{x}-\boldsymbol{y}) = 2\mu^2\Big\{\left[(1-k)(k+2\xi) - 2\xi^2\right] v^{1}_{1,11}(\boldsymbol{x}-\boldsymbol{y}) - k(1+k) v^{2}_{2,11}(\boldsymbol{x}-\boldsymbol{y})\Big\}\,, \tag{43}$$

Bigoni & Capuani [17, Appendix B] have shown that

$$\mathbb{K}_{sirg}\dot{p}^{g}_{,rs}(\boldsymbol{x}-\boldsymbol{y}) = F_{,i}(\boldsymbol{x}-\boldsymbol{y})\,, \tag{44}$$

which, applied to equation (42), allows one to eliminate the differentiation with respect to y_i, thus yielding an *integral equation for the incremental mean stress outside the inclusion, produced by the uniform inelastic field* $v^{\mathrm{P}}_{l,k}$

$$\dot{p}(\boldsymbol{y}) = -\int_{\partial D_{\mathrm{in}}} \mathbb{K}_{jklm} v^{\mathrm{P}}_{m,l} \dot{p}^{k}(\boldsymbol{x}-\boldsymbol{y}) n_j \,\mathrm{d}S_{\boldsymbol{x}} + \int_{D_{\mathrm{in}}} F(\boldsymbol{x}-\boldsymbol{y}) v^{\mathrm{P}}_{m,m}\,\mathrm{d}V_{\boldsymbol{x}}\,. \tag{45}$$

The earlier-mentioned procedure can be repeated using the expression (39) instead of (38), namely the second formulation for the displacement field, to derive an expression that is alternative, but equivalent, to (45). Equation (41) transforms into

$$\frac{\partial \dot{p}(\boldsymbol{y})}{\partial y_i} = -\int_{\partial D_{\mathrm{in}}} \mathbb{K}_{sirg}\left[\mathbb{K}_{jklm} v^{g}_{k,jrs}(\boldsymbol{x}-\boldsymbol{y}) + \dot{p}^{g}_{,rs}(\boldsymbol{x}-\boldsymbol{y})\delta_{lm}\right] v^{\mathrm{P}}_{m} n_l \,\mathrm{d}S_{\boldsymbol{x}}\,, \tag{46}$$

whereas rate equilibrium equations (1), taking account that for the Green's velocity field, $v^{g}_{k}(\boldsymbol{x}-\boldsymbol{y}) = v^{k}_{g}(\boldsymbol{x}-\boldsymbol{y})$, (see Bigoni & Capuani [17]), yield

$$\mathbb{K}_{sirg} v^{g}_{k,jrs}(\boldsymbol{x}-\boldsymbol{y}) = \mathbb{K}_{sirg} v^{k}_{g,rsj}(\boldsymbol{x}-\boldsymbol{y}) = -\dot{p}^{k}_{,ij}(\boldsymbol{x}-\boldsymbol{y})\,, \tag{47}$$

so that equation (46) becomes

$$\frac{\partial \dot{p}(\boldsymbol{y})}{\partial y_i} = \int_{\partial D_{\mathrm{in}}} \left[\mathbb{K}_{jklm}\dot{p}^{k}_{,ij}(\boldsymbol{x}-\boldsymbol{y}) - \mathbb{K}_{sirg}\dot{p}^{g}_{,rs}(\boldsymbol{x}-\boldsymbol{y}) v^{\mathrm{P}}_{m,m}\delta_{lm}\right] v^{\mathrm{P}}_{m} n_l \,\mathrm{d}S_{\boldsymbol{x}}\,. \tag{48}$$

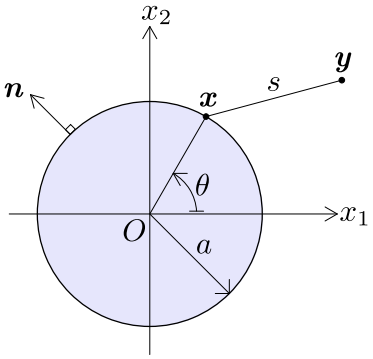

Figure 3: Reference system for the circular inclusion of radius a, subject to a transformation purely dilatational strain $v^{\mathrm{P}}_{i,j} = \beta\delta_{ij}$.

Using equation (44), we may write

$$\frac{\partial \dot{p}(\boldsymbol{y})}{\partial y_i} = \int_{\partial D_{\mathrm{in}}} \left[\mathbb{K}_{jklm}\dot{p}^k_{,ij}(\boldsymbol{x}-\boldsymbol{y}) - F_{,i}(\boldsymbol{x}-\boldsymbol{y})\delta_{lm}\right] v^{\mathrm{P}}_m n_l \,\mathrm{d}S_{\boldsymbol{x}}\,, \tag{49}$$

so that the differentiation with respect to y_i can be eliminated, thus yielding an *integral equation for the incremental mean stress outside the inclusion, produced by the uniform inelastic field* $v^{\mathrm{P}}_{l,k}$

$$\dot{p}(\boldsymbol{y}) = -\int_{\partial D_{\mathrm{in}}} \left[\mathbb{K}_{jklm}\dot{p}^k_{,j}(\boldsymbol{x}-\boldsymbol{y}) - F(\boldsymbol{x}-\boldsymbol{y})\delta_{lm}\right] v^{\mathrm{P}}_m n_l \,\mathrm{d}S_{\boldsymbol{x}}\,, \tag{50}$$

where n_i is the outward unit normal to the inclusion surface ∂D_{in}.

As a conclusion, the mechanical fields outside an inclusion of arbitrary shape, embedded in a prestressed elastic incompressible infinite matrix, can be summarized as follows:

- incremental displacement field, given by equation (25) or equation (33);
- incremental mean stress field, given by equation (45) or equation (50);
- incremental nominal stress rate field given by

$$\dot{t}_{ij}(\boldsymbol{y}) = \mathbb{K}_{ijkl}v_{l,k}(\boldsymbol{y}) + \dot{p}(\boldsymbol{y})\delta_{ij}\,, \tag{51}$$

  where equations (25) or (33) and equations (45) or (50) can be alternatively used.

2.2.3 Example: the circular inclusion

As a simple example, we consider a circular inclusion of radius a, subject to an inelastic purely volumetric dilatational Eulerian incremental strain, $v^{\mathrm{P}}_{i,j} = \beta\delta_{ij}$. With reference to the coordinate system sketched in Figure 3, we consider a source point $\boldsymbol{x}$ lying on the inclusion surface (so that $\boldsymbol{x} = \{\, a\cos\theta; a\sin\theta \,\}$) and a generic point $\boldsymbol{y}$ (outside the inclusion) at which we will calculate the displacement and mean stress fields; furthermore, the inclusion is centred at the origin O of the x_1–x_2 reference system. With these assumptions and defining the distance between the points $\boldsymbol{x}$ and $\boldsymbol{y}$ as

$$s = \sqrt{(a\cos\theta - y_1)^2 + (a\sin\theta - y_2)^2}\,, \tag{52}$$

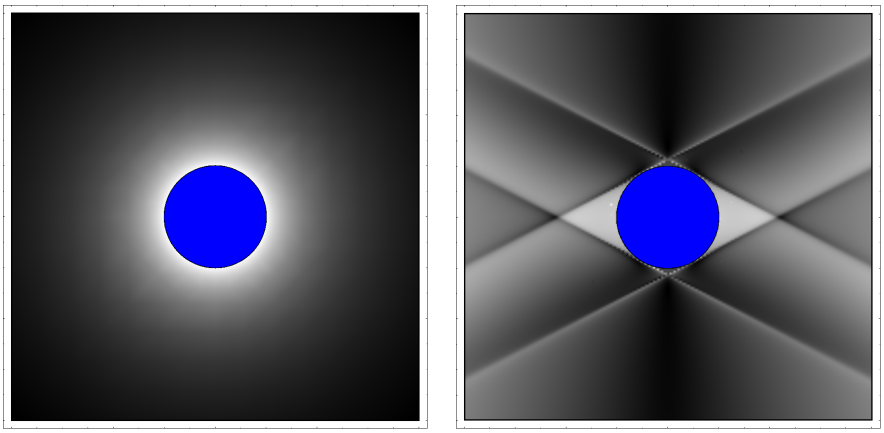

(a) *Isotropic incompressible material.* **(b)** *J_2–deformation theory of plasticity.*

Figure 4: Modulus of the incremental displacement field near a circular inclusion in an infinite medium. The inclusion has radius a and is subject to a purely dilatational strain. (**a**) Isotropic, incompressible matrix material without prestress. (**b**) J_2–deformation theory of plasticity matrix material, prestressed near the elliptic boundary ($N = 0.380$; $\widehat{\varepsilon} = 0.657$; $\widehat{\varepsilon}^{\mathrm{E}} = 0.658$); Note the strong effect of prestress, determining four localizations of deformation, parallel to the shear band inclinations corresponding to ellipticity loss.

and using equations (25) and (45), the boundary equations for *incremental displacements and mean stress around a circular inclusion in a prestressed nonlinear elastic material* become, respectively,

$$v_g(\boldsymbol{y}) = \mu\,\beta\,a\int_0^{2\pi}\left[-(k+\eta)n_1 v_1^g + (k-\eta)n_2 v_2^g\right]\mathrm{d}\theta + \beta\,a^2\int_0^{2\pi}\dot{p}^g\,\mathrm{d}\theta\,, \tag{53}$$

and

$$\dot{p}(\boldsymbol{y}) = -\mu\,\beta\,a\int_0^{2\pi}\left[-(k+\eta)n_1\dot{p}^1 + (k-\eta)n_2\dot{p}^2\right]\mathrm{d}\theta + 2\mu^2\beta\,a^2\int_0^{2\pi}\left\{\left[(1-k)(k+2\xi) - 2\xi^2\right]v^1_{1,11} - k(1+k)v^2_{2,11}\right\}\mathrm{d}\theta\,. \tag{54}$$

Equations (52) and (54) can be rewritten using equations (33) and (50) in the fully equivalent forms

$$v_g(\boldsymbol{y}) = -\mu\,\beta\,a^2\int_0^{2\pi}\left\{\left[(\xi-k-\eta)n_1^2 - \xi n_2^2\right]v^g_{1,1} + \left[(\xi+k-\eta)n_2^2 - \xi n_1^2\right]v^g_{2,2} + (2+k-\eta)n_1n_2v^g_{2,1} + (2-k-\eta)n_1n_2v^g_{1,2} + \frac{\dot{p}^g}{\mu}\right\}\mathrm{d}\theta\,, \tag{55}$$

and

$$\dot{p}(\boldsymbol{y}) = -\mu\,\beta\,a^2\int_0^{2\pi}\left\{\left[(\xi-k-\eta)n_1^2 - \xi n_2^2\right]\dot{p}^1_{,1} + \left[(\xi+k-\eta)n_2^2 - \xi n_1^2\right]\dot{p}^2_{,2} + (2+k-\eta)n_1n_2\dot{p}^2_{,1} + (2-k-\eta)n_1n_2\dot{p}^1_{,2} - \frac{F}{\mu}\right\}\mathrm{d}\theta\,. \tag{56}$$

Equation (53) has been used to generate the incremental solution shown in Figure 4, for an isotropic elastic (with null prestress) matrix material (on the left) and for a J_2–deformation theory matrix material uniformly deformed near the boundary (but still within) the elliptic region.

The latter material, with a hardening exponent $N = 0.380$, is pre-deformed at a logarithmic strain $\widehat{\varepsilon} = 0.657$, a value close to loss of ellipticity, occurring at $\widehat{\varepsilon}^{\mathrm{E}} = 0.658$.

The strong effect of prestress is evident from Figure 4, so that *the incremental displacement fields are completely different* and the situation near the ellipticity loss shows the emergence of strongly localized fields, focussed parallel to the four shear band directions (for a J_2–material with $N = 0.380$ the shear bands are inclined at $\pm 27.37°$ with respect to the x_1–axis).

In the simple case of null prestress, $k = 0$ and $\eta = 0$, equations (53) and (54) reduce to

$$v_g(\boldsymbol{y}) = -\beta\, a^2 \int_0^{2\pi} \dot{p}^g \,\mathrm{d}\theta\,, \qquad \dot{p}(\boldsymbol{y}) = 4\mu^2 \beta\, a^2 \xi(1-\xi) \int_0^{2\pi} v^1_{1,11}\,\mathrm{d}\theta\,, \tag{57}$$

so that introducing isotropy, $\xi = 1$, they become

$$v_g(\boldsymbol{y}) = \frac{\beta\, a^2}{2\pi} \int_0^{2\pi} \frac{y_g - x_g}{s^2}\,\mathrm{d}\theta\,, \qquad \dot{p}(\boldsymbol{y}) = 0\,, \tag{58}$$

and the velocity can be evaluated as

$$v_g(\boldsymbol{y}) = \frac{\beta\, a^2}{2} \frac{y_g}{y_1^2 + y_2^2}\,. \tag{59}$$

We can note that the last expression can be written in a polar coordinate system, which yields only a radial velocity field,

$$v_r(r) = \frac{\beta\, a^2}{2\, r}\,, \qquad v_\theta(r) = 0\,, \tag{60}$$

where $r = \sqrt{y_1^2 + y_2^2}$, namely the same result of linear elasticity (the so-called Lamé solution).

3 Edge dislocations in prestressed elastic materials

The integral equations determining the incremental displacement and mean stress for a straight edge dislocation can be obtained from equations (33) and (50) by considering a thin (thickness h) rectangular inclusion (without loss of generality) with one edge centred at the origin of the x_1–x_2 axes, and subject to the incremental simple shear displacement field,

$$v_i^{\mathrm{P}} = \frac{x_k n_k}{h}\, b_i\,, \qquad b_k n_k = 0\,, \tag{61}$$

where n_k is the unit vector orthogonal and b_k is a vector parallel to the long edges of the rectangle. Note that the modulus of $\boldsymbol{b}$ is twice the maximum displacement induced by the simple shear inside the rectangle. The incremental displacement field (61) satisfies

$$v^{\mathrm{P}}_{k,k} = 0\,, \qquad \delta_{lm} v^{\mathrm{P}}_m n_l = 0\,, \tag{62}$$

so that inserting equation (61) into equations (33) and (50) and taking the limit $h \to 0$, we obtain *the integral equations for a straight edge dislocation in a prestressed material*,

$$v_g(\boldsymbol{y}) = \int_L b_m n_l(\boldsymbol{x}) \mathbb{K}_{jklm} v^g_{k,j}(\boldsymbol{x} - \boldsymbol{y})\,\mathrm{d}l_{\boldsymbol{x}}\,, \tag{63a}$$

$$\dot{p}(\boldsymbol{y}) = -\int_L b_m n_l(\boldsymbol{x}) \mathbb{K}_{jklm} \dot{p}^k_{,j}(\boldsymbol{x} - \boldsymbol{y})\,\mathrm{d}l_{\boldsymbol{x}}\,, \tag{63b}$$

where L is the dislocation line of unit normal n_i and b_i is the (constant) Burgers vector, defining the jump in the incremental displacement imposed across the dislocation, see Figure 5.

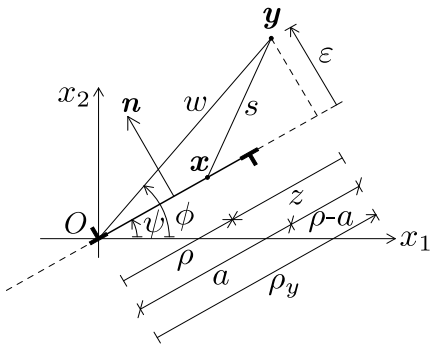

Figure 5: Infinite medium, including a straight *edge dislocation dipole* of finite length a and inclined at a constant angle ψ with respect to the x_1–axis.

We consider a straight edge dislocation dipole with one of the two dislocations centred at the origin of the x_1–x_2 reference system, a generic source point $\boldsymbol{x}$ lying on the dislocation line (so that $\boldsymbol{x} = \{\, \rho\cos\psi, \rho\sin\psi \,\}$) and a generic point $\boldsymbol{y}$ at which we will calculate the displacement and mean stress fields, as shown in Figure 6. Representing the dislocation line with a polar coordinate system (ρ, ψ), where $\rho \in [0, a]$, the Burgers vector $\boldsymbol{b}$ and the normal vector $\boldsymbol{n}$ become

$$\boldsymbol{b} = b\,\{\,\cos\psi, \sin\psi\,\}\,, \qquad \boldsymbol{n} = \{\,-\sin\psi, \cos\psi\,\}\,, \tag{64}$$

whereas the distance between the points $\boldsymbol{x}$ and $\boldsymbol{y}$ is defined as

$$s = |\boldsymbol{x} - \boldsymbol{y}| = \sqrt{(\rho\cos\psi - y_1)^2 + (\rho\sin\psi - y_2)^2}\,. \tag{65}$$

similar to the circular inclusion example.

Because $\boldsymbol{b}$ is constant and orthogonal to $\boldsymbol{n}$, the incremental displacement and mean stress fields for *an edge dislocation dipole* can be obtained, respectively, in the following form:

$$v_g(\boldsymbol{y},\psi) = \mu b \int_0^a \left[\Omega_1(\psi)\, v^g_{1,1}(\boldsymbol{y},\psi,\rho) + \Omega_2(\psi)\, v^g_{1,2}(\boldsymbol{y},\psi,\rho) + \Omega_3(\psi)\, v^g_{2,1}(\boldsymbol{y},\psi,\rho)\right] \mathrm{d}\rho\,, \tag{66a}$$

$$\begin{aligned}\dot{p}(\boldsymbol{y},\psi) = -\mu b \int_0^a \big[&\Omega_2(\psi)\, \dot{p}^1_{,2}(\boldsymbol{y},\psi,\rho) + \Omega_3(\psi)\, \dot{p}^2_{,1}(\boldsymbol{y},\psi,\rho) + \Omega_4(\psi)\, \dot{p}^1_{,1}(\boldsymbol{y},\psi,\rho) \\ &+ \Omega_5(\psi)\, \dot{p}^2_{,2}(\boldsymbol{y},\psi,\rho)\big]\, \mathrm{d}\rho\,,\end{aligned} \tag{66b}$$

where

$$\begin{aligned}&\Omega_1(\psi) = (\eta - 2\xi)\sin(2\psi)\,, && \Omega_2(\psi) = (1-k)\cos^2\psi - (1-\eta)\sin^2\psi\,,\\ &\Omega_3(\psi) = (1-\eta)\cos^2\psi - (1+k)\sin^2\psi\,, && \Omega_4(\psi) = \frac{1}{2}(k + \eta - 2\xi)\sin(2\psi)\,,\\ &\Omega_5(\psi) = \frac{1}{2}(k - \eta + 2\xi)\sin(2\psi)\,.\end{aligned} \tag{67}$$

3.1 The edge dislocation solution along the dipole line

The displacement and the mean stress fields can be explicitly evaluated along the dislocation line through equations (66) and the following considerations on the Green's function structure. From Figure 5, the point $\boldsymbol{y}$, when taken along the dislocation line, is represented by $\boldsymbol{y} = (\rho + z)\,\{\,\cos\psi, \sin\psi\,\}$ and the angle ϕ is constant and equal to ψ. In this case, we have that $s = z = \rho_y - \rho$ because $\varepsilon = 0$ along the dislocation line. This constraint allows us to express the

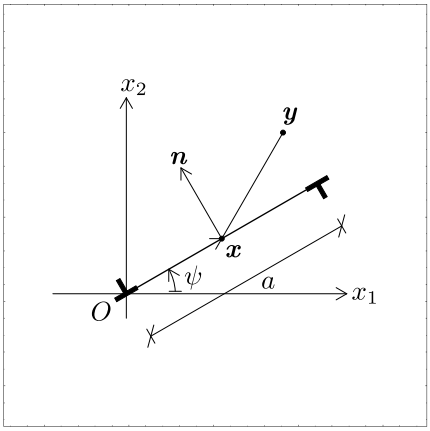

(a) *Dipole reference system and geometry.*

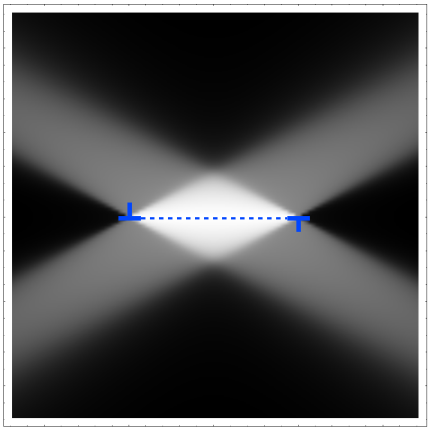

(b) $\psi = 0, \quad N = 0.363, \quad \widehat{\varepsilon} = 0.610.$

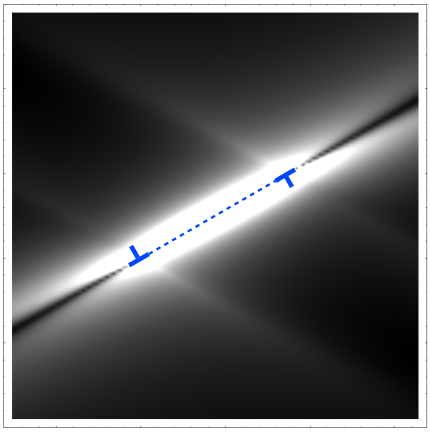

(c) $\psi = \pi/6, \quad N = 0.363, \quad \widehat{\varepsilon} = 0.610.$

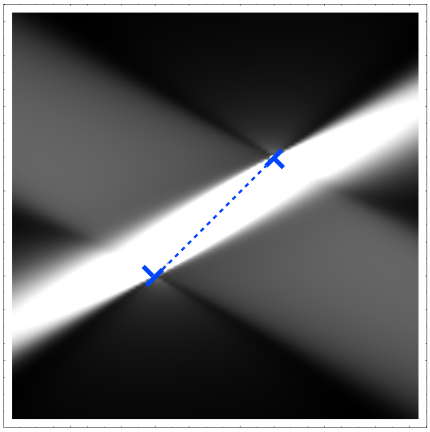

(d) $\psi = \pi/4, \quad N = 0.363, \quad \widehat{\varepsilon} = 0.610.$

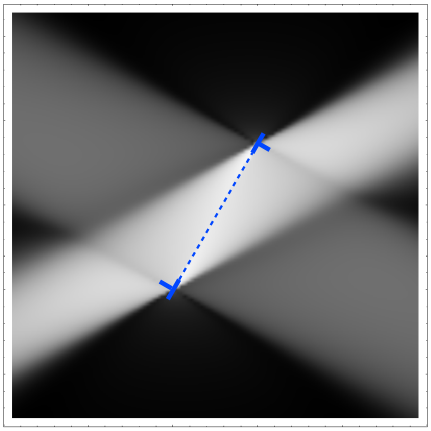

(e) $\psi = \pi/3, \quad N = 0.363, \quad \widehat{\varepsilon} = 0.610.$

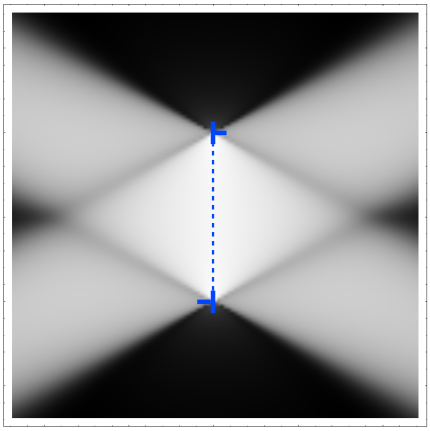

(f) $\psi = \pi/2, \quad N = 0.363, \quad \widehat{\varepsilon} = 0.610.$

Figure 6: The (level sets of the modulus of incremental) displacement field produced by *the emission of a straight edge dislocation dipole* (of length a and inclination ψ with respect to the x_1–axis of orthotropy, see the geometrical setting in (**a**)) in a (J_2–deformation theory) plastic material, homogeneously deformed until near the elliptic boundary.

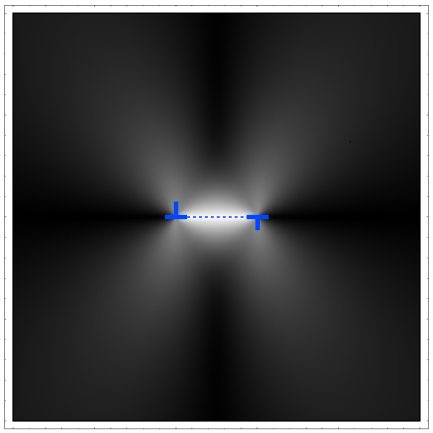

Figure 7: The (level sets of the modulus of the) displacement field around an edge dislocation dipole in an infinite, incompressible elastic and isotropic medium (without prestress). Note the strong difference with the behaviour near the elliptic threshold (Figure 6).

Green's function gradient for displacement and mean stress as

$$v^g_{i,j}(s,\psi) = \frac{1}{s}\,\bar{v}^g_{i,j}(\psi)\,, \qquad \dot{p}^g_{,i}(s,\psi) = \frac{1}{s^2}\,\dot{\bar{p}}^g_{,i}(\psi)\,, \tag{68}$$

where $\bar{v}^g_{i,j}$ and $\dot{\bar{p}}^g_{,i}$ are function of the sole variable ψ. Now the integration along ρ can be performed because, in equation (68), the dependence on s is explicit, so that the incremental displacement and mean stress fields along the dislocation take the following form:

$$v_g(\rho_y,\psi) = b\log\left(\frac{\rho_y}{\rho_y - a}\right)\Big[\Omega_1(\psi)\,\bar{v}^g_{1,1}(\psi) + \Omega_2(\psi)\,\bar{v}^g_{1,2}(\psi) + \Omega_3(\psi)\,\bar{v}^g_{2,1}(\psi)\Big]\,, \tag{69a}$$

$$\dot{p}(\rho_y,\psi) = \frac{b\,a}{\rho_y(\rho_y - a)}\Big[\Omega_2(\psi)\,\dot{\bar{p}}^1_{,2}(\psi) + \Omega_3(\psi)\,\dot{\bar{p}}^2_{,1}(\psi) + \Omega_4(\psi)\,\dot{\bar{p}}^1_{,1}(\psi) + \Omega_5(\psi)\,\dot{\bar{p}}^2_{,2}(\psi)\Big]\,. \tag{69b}$$

Note that the incremental displacement and mean stress fields exhibit essentially different asymptotic behaviours at the dislocation tips (near both points, $\rho_y = 0$ and $\rho_y = a$). In fact, as one can expect, the displacement field shows a logarithmic singularity (similar to that found by Eshelby [3]), whereas the mean stress displays a $1/s$ singularity.

3.2 A curiosity on the incompressible isotropic linear elastic solution

In the simple case of null prestress, $k = 0$ and $\eta = 0$, equations (66) reduce to

$$v_g(\boldsymbol{y}) = \mu\,b\int_0^a \Big\{-2\xi\,v^g_{1,1}(\boldsymbol{y},\psi,\rho)\sin(2\psi) + \big[v^g_{1,2}(\boldsymbol{y},\psi,\rho) + v^g_{2,1}(\boldsymbol{y},\psi,\rho)\big]\cos(2\psi)\Big\}\,\mathrm{d}\rho\,, \tag{70a}$$

$$\dot{p}(\boldsymbol{y}) = -\mu\,b\int_0^a \Big\{\big[\dot{p}^1_{,2}(\boldsymbol{y},\psi,\rho) + \dot{p}^2_{,1}(\boldsymbol{y},\psi,\rho)\big]\cos(2\psi) - \xi\big[\dot{p}^1_{,1}(\boldsymbol{y},\psi,\rho) - \dot{p}^2_{,2}(\boldsymbol{y},\psi,\rho)\big] \times \sin(2\psi)\Big\}\,\mathrm{d}\rho\,, \tag{70b}$$

so that introducing isotropy, $\xi = 1$, and considering an edge dislocation dipole aligned to the x_1–axis, $\psi = 0$, they become

$$v_g(\boldsymbol{y}) = \mu b \int_0^a \left[v^g_{1,2}(\boldsymbol{y}, \rho) + v^g_{2,1}(\boldsymbol{y}, \rho) \right] \mathrm{d}\rho \,, \tag{71a}$$

$$\dot{p}(\boldsymbol{y}) = -\mu b \int_0^a \left[\dot{p}^1_{,2}(\boldsymbol{y}, \rho) + \dot{p}^2_{,1}(\boldsymbol{y}, \rho) \right] \mathrm{d}\rho \,. \tag{71b}$$

The integration of equations (71) can be performed in an explicit way, thus yielding

$$v_1(\boldsymbol{y}) = \frac{b}{2\pi} \left[\arctan\left(\frac{y_2}{y_1 - x_1} \right) + \frac{(y_1 - x_1)\, y_2}{(y_1 - x_1)^2 + y_2^2} \right]_{x_1=0}^{x_1=a} , \tag{72a}$$

$$v_2(\boldsymbol{y}) = -\frac{b}{4\pi} \left[\frac{(y_1 - x_1)^2 - y_2^2}{(y_1 - x_1)^2 + y_2^2} \right]_{x_1=0}^{x_1=a} , \tag{72b}$$

$$\dot{p}(\boldsymbol{y}) = -\frac{\mu b y_2}{\pi} \left[\frac{1}{(y_1 - x_1)^2 + y_2^2} \right]_{x_1=0}^{x_1=a} . \tag{72c}$$

Equations (72) coincide with the linear elastic (compressible) solution for a dislocation [2], when taken with Poisson's ratio equal to $1/2$.

An issue of interest is that the logarithmic behaviour near the the dislocation tip is not present in the incompressibility limit, so that a singular stress field is generated by a displacement field not showing the usual logarithmic singularity.

4 The numerical treatment of the boundary integral equations

The numerical treatment of the boundary integral equations (66) involves a Cauchy-type integral, for equation (66a), and a hypersingular integral, for equation (66b). The use of these equations implies the knowledge of the gradient of the Green's function for incremental displacement and for incremental in-plane mean stress; the former has been given by Bigoni & Capuani [17] and will not be repeated, while the latter can be obtained using equations (48) and (62) given by Bigoni & Capuani [17], so that we arrive at the final expressions

$$\begin{aligned} \dot{p}^g_{,j} = {} & \frac{1}{2\pi s^4} \left[1 - \frac{k}{1+k} \frac{1}{\gamma_1^{\delta_{1g}} \sqrt{-\gamma_2} + \gamma_2^{\delta_{1g}} \sqrt{-\gamma_1}} \right] \\ & \times \left\{ (\delta_{1g}\delta_{1j} - \delta_{2g}\delta_{2j}) \left[(x_1 - y_1)^2 - (x_2 - y_2)^2 \right] + 2(\delta_{1g}\delta_{2j} + \delta_{2g}\delta_{1j})(x_1 - y_1)(x_2 - y_2) \right\} \\ & + \frac{1}{2\pi^2(1+k)} \int_0^{\pi} \zeta_{gj}(\boldsymbol{x}, \boldsymbol{y}, \alpha)\, \mathrm{d}\alpha + \frac{k}{\pi^2(1+k)} \int_0^{\frac{\pi}{2}} \Xi_{gj}(\boldsymbol{x}, \boldsymbol{y}, \alpha)\, \mathrm{d}\alpha \,, \end{aligned} \tag{73}$$

where $\zeta_{gj}(\boldsymbol{x}, \boldsymbol{y}, \alpha)$ and $\Xi_{gj}(\boldsymbol{x}, \boldsymbol{y}, \alpha)$ are functions (not reported for brevity) of the distance between the source point $\boldsymbol{x}$, the generic point $\boldsymbol{y}$ and the angle α, as defined by Bigoni & Capuani [17, Figure 1]; coefficients γ_1 and γ_2 are also defined in Bigoni & Capuani [17, equation (15)]. Note also that δ_{1g}, δ_{2g}, δ_{1j} and δ_{2j} are all Kronecker deltas (taking the values 0 and 1). Note that the term $\zeta_{gj}(\boldsymbol{x}, \boldsymbol{y}, \alpha)$ is related to the gradient of the Green's hydrostatic nominal stress, whereas the term $\Xi_{gj}(\boldsymbol{x}, \boldsymbol{y}, \alpha)$ is related to the second gradient of the Green's velocity.

The numerical evaluation of the boundary integral equation (66a) requires the following treatment. First, we introduce the reference system shown in Figure 5, where

$$\boldsymbol{x} = \{ \rho \cos\psi, \rho \sin\psi \} \,, \qquad \boldsymbol{y} = \{ w \cos\phi, w \sin\phi \} \,, \tag{74}$$

and

$$\phi = \arctan\left(\frac{y_2}{y_1}\right), \qquad w = \sqrt{y_1^2 + y_2^2}, \tag{75}$$

so that

$$y_1 - x_1 = (\rho_y - \rho)\cos\psi - \varepsilon\sin\psi, \qquad y_2 - x_2 = (\rho_y - \rho)\sin\psi + \varepsilon\cos\psi, \tag{76}$$

where ε can become a small parameter, and

$$\varepsilon = w\sin(\phi - \psi), \qquad \rho_y = w\cos(\phi - \psi). \tag{77}$$

We introduce the change of variables

$$z = \rho_y - \rho, \tag{78}$$

so that

$$y_1 - x_1 = z\cos\psi - \varepsilon\sin\psi, \qquad y_2 - x_2 = z\sin\psi + \varepsilon\cos\psi. \tag{79}$$

Note from Figure 5 that, whereas the source point $\boldsymbol{x}$ ranges along the dislocation line $\rho \in [0, a]$, point $\boldsymbol{y}$ is arbitrary. Therefore the variable z (does not) vanishes for all $\boldsymbol{y}$ whose projections lie (out-) in-side the dislocation line ($\rho_y \notin (0, a)$) $\rho_y \in (0, a)$, so that the problem in managing equations (66) occurs when $\rho_y \in (0, a)$. In this situation, ε can be made arbitrarily small, but different from zero, whereas variable z can be expanded around zero.

Using (78), the integrals involved in (66a) can be written in the following form:

$$\tilde{v} = \int_{\rho_y - a}^{\rho_y} \frac{z \pm \varepsilon}{z^2 + \varepsilon^2}\, G(\varepsilon, z)\, \mathrm{d}z, \tag{80}$$

where

$$G(\varepsilon, z) = \int_0^{\frac{\pi}{2}} \Delta(\varepsilon, z, \alpha)\, \mathrm{d}\alpha, \tag{81}$$

in which function $\Delta(\varepsilon, z, \alpha)$ takes a complicated expression, not reported for brevity.

Therefore, a Taylor series expansion of function $\Delta(\varepsilon, z, \alpha)$ in the variable z yields

$$\Delta(\varepsilon, z, \alpha) = \tilde{\Delta}(\varepsilon, z, \alpha) + O(z^2), \tag{82}$$

where

$$\tilde{\Delta}(\varepsilon, z, \alpha) = \Delta(\varepsilon, 0, \alpha) + \left.\frac{\partial \Delta(\varepsilon, z, \alpha)}{\partial z}\right|_{z=0} z, \tag{83}$$

so that function $G(\varepsilon, z)$ can be regularized as

$$G(\varepsilon, z) = \int_0^{\frac{\pi}{2}} \left[\Delta(\varepsilon, z, \alpha) - \tilde{\Delta}(\varepsilon, z, \alpha)\right] \mathrm{d}\alpha + \int_0^{\frac{\pi}{2}} \Delta(\varepsilon, 0, \alpha)\, \mathrm{d}\alpha + z\int_0^{\frac{\pi}{2}} \left.\frac{\partial \Delta(\varepsilon, z, \alpha)}{\partial z}\right|_{z=0} \mathrm{d}\alpha, \tag{84}$$

where the derivative of function $\Delta(\varepsilon, z, \alpha)$ in the variable z can be easily calculated (though it takes a complicated expression, which is not reported for conciseness).

As a conclusion, instead of with the integral (80), we can work with its regularized version,

written as

$$\tilde{v}(\varepsilon,\rho_y)=\int_{\rho_y-a}^{\rho_y}\frac{z\pm\varepsilon}{z^2+\varepsilon^2}\left\{\int_0^{\frac{\pi}{2}}\left[\Delta(\varepsilon,z,\alpha)-\tilde{\Delta}(\varepsilon,z,\alpha)\right]\mathrm{d}\alpha\right\}\mathrm{d}z$$
$$+\left[\pm\arctan\left(\frac{z}{\varepsilon}\right)+\log\sqrt{z^2+\varepsilon^2}\right]_{z=\rho_y-a}^{z=\rho_y}\int_0^{\frac{\pi}{2}}\Delta(\varepsilon,0,\alpha)\,\mathrm{d}\alpha$$
$$+\left[z-\varepsilon\arctan\left(\frac{z}{\varepsilon}\right)\pm\varepsilon\log\sqrt{z^2+\varepsilon^2}\right]_{z=\rho_y-a}^{z=\rho_y}\int_0^{\frac{\pi}{2}}\left.\frac{\partial\Delta(\varepsilon,z,\alpha)}{\partial z}\right|_{z=0}\mathrm{d}\alpha\,, \quad (85)$$

in which the singular terms have been explicitly evaluated. The integral equation for in-plane mean stress increment (66b) can be treated in a way similar to that used to obtain (85), which is used in Section 5 to produce numerical values for the incremental displacement fields near a dislocation dipole.

5 Dislocation clustering in a metal near the elliptic border

We are now in a position to explore the effect of prestress on a metal deformed near the elliptic boundary. For this purpose, we can use equation (66a) in the regularized version (85) for an edge dislocation dipole (which may be thought of as a 'super dislocation', i.e. a collection of dislocations smeared out along a certain direction) of length a, which is assumed to be nucleated in a J_2–deformation theory material with a hardening parameter $N=0.363$ (see equations (9) and (10)). Incremental displacement fields for a unit length Burgers vector, at a prestrain $\widehat{\varepsilon}=0.610$ (so that the material is close to the ellipticity threshold $\widehat{\varepsilon}^{\mathrm{E}}=0.642$, but still within the elliptic region) are plotted in Figure 6 for different inclinations ψ of the dipole with respect to the orthotropy axes (see the sketch in Figure 6a).

Note that the dislocation solution depends on the parameter η, which has been assumed equal to 0.490. The following inclinations have been considered: $\psi=\{\,0,\pi/6,\pi/4,\pi/3,\pi/2\,\}$.

It may be worth observing that the perturbation induced by a dislocation dipole is different from that induced by a force dipole (as considered by Bigoni & Capuani [17]). In fact force and dislocation dipoles can produce similar effects only in the far fields and only under the assumption that the prestress is absent [14].

In all cases reported in Figure 6, we observe the formation of zones of intense deformation, aligned parallel to the inclination of the shear bands ($\pm27.37°$ with respect to the x_1–axis), formally possible only at loss of ellipticity. The response of the material far from the elliptic boundary is completely different, as shown in Figure 7, pertaining to an isotropic incompressible material at null prestress.

Because the dislocation activity is triggered by a rise in the shear stress, and this occurs for highly prestressed materials along the preferred directions shown in Figure 6, along these the dislocation activity tends to be strongly promoted. Therefore, this activation will again generate an increment in shear stress along the same directions, thus producing a sort of 'cascade effect', which will cluster dislocation formation along shear bands. This effect may explain the fact that the amount of slip taking place on active shear bands may be up to three orders of magnitude greater than that produced by a single dislocation [13].

6 Conclusions

Prestress has been shown to be an important factor in the mechanics of dislocation clustering, in ductile metals deformed near the shear band formation. A new solution for an edge dislo-

cation, valid for incremental nonlinear elasticity, with the current state taken as homogeneous, shows in fact emergence of highly localized deformation patterns, when the material is deformed near the boundary of ellipticity loss, which may trigger 'cascade' dislocation activation along shear band directions. Although this conclusion is limited by the assumption of homogeneity of the prestress (which is the only way to arrive at analytical solutions), it may correctly model the situation when a dislocation dipole is emitted.

Acknowledgments

Partial support from ICMS (Edinburgh, 2010) is acknowledged. D.B. and L.P.A. gratefully acknowledge partial support from Italian Prin 2009 (prot. 2009XWLFKW-002); G.M. acknowledges support from the FP7 research project PIAP-GA-2011-286110.

A Notes on the photoelastic experiment reported in Figure 1

Photoelastic experiments have been performed with a circular (with quarterwave retarders for $560\,\mathrm{nm}$) polariscope (dark field arrangement and equipped with a white and sodium vapor lightbox at $\lambda = 589.3\,\mathrm{nm}$, purchased from Tiedemann & Betz), designed by us and manufactured at the University of Trento (see `http://www.ing.unitn.it/dims/ssmg/`). Photos have been taken with a Nikon D200 digital camera equipped with a AF-S micro Nikkor (70-180 mm, 1:4.55.6D) lens. The photoelastic material is a $5\,\mathrm{mm}$ thick platelet obtained from a commercial two-part epoxy resin (Crystal Resins© by Gedeo, 305 Avenue du pic de Bretagne, 13420 Gemenos, France). The orthotropic material has been obtained by cutting (with a circular saw, blade HSS-DMo5 $63\times0.3\times16$ Z128 A) $0.3\,\mathrm{mm}$ thick and $2\,\mathrm{mm}$ deep parallel grooves (at a distance $2.5\,\mathrm{mm}$) in the resin sample, a technique previously used by O'Regan [19] on photoelastic coatings. The dislocation has been created with two $0.5\,\mathrm{mm}$ thick steel platelets in contact to each other at one side and attached to the resin on the other side. The platelets (placed horizontally and aligned parallel to the dashed line in Figure 1) have been forced to slide each against the other to generate the stress field near an edge dislocation.

Bibliography

[1] J.D. Eshelby. "The continuum theory of lattice defects". In: *Solid State Phys.* 3.C (1956), pp. 79–144. DOI: 10.1016/S0081-1947(08)60132-0 (cit. on p. 1).

[2] J.D. Eshelby. "The determination of the elastic field of an ellipsoidal inclusion, and related problems". In: *Proc. Royal Soc. A* 241.1226 (1957), pp. 376–396. DOI: 10.1098/rspa.1957.0133 (cit. on pp. 1, 2, 4, 15).

[3] J.D. Eshelby. "A simple derivation of the elastic field of an edge dislocation". In: *British Journal of Applied Physics (B.J.A.P.)* 17.9 (1966), pp. 1131–1135. DOI: 10.1088/0508-3443/17/9/303 (cit. on pp. 1, 14).

[4] J.R. Willis. "Dislocations and inclusions". In: *J. Mech. Phys. Solids* 13.6 (1965). Ed. by Pergamon Press Ltd., pp. 377–395. DOI: 10.1016/0022-5096(65)90038-4 (cit. on pp. 1, 2, 4, 7).

[5] F. Dal Corso and D. Bigoni. "Growth of slip surfaces and line inclusions along shear bands in a softening material". In: *Int. J. Fracture* 166.1-2 (2010), pp. 225–237. DOI: 10.1007/s10704-010-9534-1. URL: http://www.ing.unitn.it/~bigoni/paper/slip_surfaces_shear_bands_softening_dalcorso_bigoni.pdf (cit. on p. 1).

[6] V. Mantič and F. Paris. "Symmetrical representation of stresses in the Stroh formalism and its application to a dislocation and a dislocation dipole in an anisotropic elastic medium". In: *J. Elasticity* 47.2 (1997), pp. 101–120. DOI: 10.1023/A:1007400325896 (cit. on p. 1).

[7] J.W. Steeds and J.R. Willis. "Dislocations in anisotropic media". In: *Dislocations in Solids* 1 (1979). Ed. by F.R.N. Nabarro. New York, NY: North-Holland, pp. 143–166 (cit. on p. 1).

[8] T.C.T. Ting. "Green's functions for a bimaterial consisting of two orthotropic quarter planes subjected to an antiplane force and a screw dislocation". In: *Math. Mech. Solids* 10.2 (2005), pp. 197–211. DOI: 10.1177/1081286505036318 (cit. on p. 1).

[9] W. Cai et al. "Anisotropic elastic interactions of a periodic dislocation array". In: *Phys. Rev. Letters* 86.25 (2001), pp. 5727–5730. DOI: 10.1103/PhysRevLett.86.5727 (cit. on p. 1).

[10] E. Clouet, L. Ventelon, and F. Willaime. "Dislocation core energies and core fields from first principles". In: *Phys. Rev. Letters* 102.5 (2009). DOI: 10.1103/PhysRevLett.102.055502 (cit. on p. 1).

[11] J.W. Hutchinson and K.W. Neale. "Finite strain J_2-deformation theory". In: *Proc. IUTAM Symp. on Finite Elasticity*. Ed. by D. E. Carlson and R.T. Shield. The Hague, The Netherlands: Martinus Nijhoff, 1979, pp. 237–247. DOI: 10.1007/978-94-009-7538-5_14 (cit. on pp. 1, 3).

[12] J.W. Hutchinson and V. Tvergaard. "Shear band formation in plane strain". In: *Int. J. Solids Structures* 17.5 (1981), pp. 451–470. DOI: 10.1016/0020-7683(81)90053-6 (cit. on p. 1).

[13] A.H. Cottrell. *Dislocations and plastic flow in crystals*. Oxford, UK: Oxford University Press, 1953 (cit. on pp. 2, 17).

[14] D. Bigoni. *Nonlinear solid mechanics. Bifurcation theory and material instability*. Cambridge, UK: Cambridge University Press, 2012 (cit. on pp. 2, 3, 17).

[15] M.A. Biot. *Mechanics of incremental deformations*. New York, NY: John Wiley and Sons, 1965 (cit. on p. 3).

[16] D. Bigoni and F. Dal Corso. "The unrestrainable growth of a shear band in a prestressed material". In: *Proc. Royal Soc. A* 464.2097 (2008), pp. 2365–2390. DOI: 10.1098/rspa.2008.0029. URL: http://www.ing.unitn.it/~bigoni/paper/bigoni-dalcorso_ultimissima.pdf (cit. on p. 3).

[17] D. Bigoni and D. Capuani. "Green's function for incremental nonlinear elasticity: shear bands and boundary integral formulation". In: *J. Mech. Phys. Solids* 50.3 (2002), pp. 471–500. DOI: 10.1016/S0022-5096(01)00090-4. URL: http://www.ing.unitn.it/~bigoni/paper/jmps2002-471.pdf (cit. on pp. 5, 6, 8, 15, 17).

[18] D. Bigoni et al. "A novel boundary element approach to time-harmonic dynamics of incremental non-linear elasticity: the role of pre-stress on structural vibrations and dynamic shear banding". In: *Comp. Methods Appl. Mech. Eng.* 196.41-44 (2007), pp. 4222–4249. DOI: 10.1016/j.cma.2007.04.013. URL: http://www.ing.unitn.it/~bigoni/paper/bigoni_capuani_bonetti_colli.pdf (cit. on p. 7).

[19] O'Regan R. "New method for determining strain on the surface of a body with photoelastic coatings". In: *Experimental Mech.* 5.8 (1965), pp. 241–246. DOI: 10.1007/BF02327147 (cit. on p. 18).